Available online at www.sciencedirect.com
SCIENCE DIRECT®
Chemical Physics Letters 396 (2004) 353–358
CHEMICAL PHYSICS LETTERS
www.elsevier.com/locate/cplett

An interesting magnetic behavior in molecular solid containing one-dimensional Ni(III) chain

Chunlin Ni [a], Dongbin Dang [a], You Song [a], Song Gao [b], Yizhi Li [a], Zhaoping Ni [a], Zhengfang Tian [a], Lili Wen [a], Qingjin Meng [a,*]

[a] *State Key Laboratory of Coordination Chemistry, Department of Chemistry, Coordination Chemistry Institute, Nanjing University, Hankou Road 22, Nanjing, Jiangsu 210093, PR China*

[b] *State Key Laboratory of Rare Earth Materials Chemistry and Applications, Peking University, Beijing 100871, PR China*

Received 26 June 2004; in final form 16 August 2004

Abstract

The preparation, crystal structure and magnetic properties of a new ion-pair complex, $[BrFBzNH_2Py][Ni(mnt)_2]$ (**1**) [$BrFBzNH_2Py^+$ = 1-(4′-bromo-2′-flurobenzyl)-4-aminopyridinium, mnt^{2-} = maleonitriledithiolate] are reported. The $Ni(mnt)_2^-$ anions and $[BrFBzNH_2Py]^+$ cations of **1** form completely segregated uniform stacking columns. The intrachain Ni···Ni separation is 4.045 Å in the $Ni(mnt)_2^-$ stacking column. Magnetic susceptibility measurements for **1** in the temperature range 2.0–300 K show the occurrence of significant ferromagnetic interaction in the high-temperature phase (HT), spin gap in the low-temperature phase (LT) and weak ferromagnetism due to spin canting below 5 K.

1. Introduction

The design of new molecule-based magnets with higher critical temperatures T_c has been one of the major challenges in magneto-chemistry [1,2]. Recently, bis-1,2-dithiolene transition metal complexes have attracted intensive interest because of their attractive properties and application in many fields [3,4]. The ion-pair complexes which are comprised of organic or inorganic cations and anions have a unique position in this field. One class of these complexes is exemplified by $[Ni(mnt)_2]$ complexes [5–7]. Especially, the discovery in 1996 of the ferromagnetic complex containing $Ni(mnt)_2^-$ ion, $NH_4 \cdot Ni(mnt)_2 \cdot H_2O$, revived the interest in $Ni(mnt)_2$ complexes as building blocks for new molecular magnets [8]. Recently, much of our attention has been directed at a new class of ion-pair complexes $[RbzPy]^+[Ni(mnt)_2]^-$ ($[RbzPy]^+$ = derivatives of benzylpyridinium). These efforts are motivated by the desire to tune the stacking pattern of $Ni(mnt)_2^-$ complexes, and modulate the magnetic properties by the molecular conformation of the attractive $RbzPy^+$ cation. Versatile magnetic properties, such as magnetic transition from ferromagnetic coupling to diamagnetism, meta-magnetism, ferromagnetic ordering at low temperature, and Spin-Peierls-like transitions, had been founded in our pervious Letters [9,10]. With the view to further determine the structure-function relationship for this new class of magnetic materials, in this contribution we wish to report the synthesis, crystal structure, and magnetic properties of a novel ion-pair complex $[BrFBzNH_2Py][Ni(mnt)_2]$ (**1**) which exhibits a complicated magnetic transition from ferromagnetic interaction to spin gap, then to spin canting, as the temperature is lowered.

* Corresponding author. Fax: +86 25 83314502.
E-mail address: njuchem1024@163.com (Q. Meng).

0009-2614/$ - see front matter © 2004 Elsevier B.V. All rights reserved.
doi:10.1016/j.cplett.2004.08.060

2. Experimental

[1-(4′-bromo-2′-flurobenzyl)]-4-aminopyridinium bromide was prepared by literature method [11]. A similar method for preparing $[Bu_4N][Ni(mnt)_2]$ was used to prepare $[BrFBzNH_2Py]_2[Ni(mnt)_2]$ [12]. A acetone solution (10 cm^3) of I_2 (160 mg, 0.62 mmol) was slowly added to a acetone solution (50 cm^3) of $[BrFBzNH_2Py]_2[Ni(mnt)_2]$ (903 mg,1 mmol) and the mixture was stirred for 1 h. MeOH (90 cm^3) was then added, and the mixture allowed to stand overnight; The resulting black micro-crystals of **1** formed were filtered off, washed with *i*-PrOH and dried in vacuo. Yield 480 mg, 77.2%. Anal. Calc: for $C_{20}H_{11}N_6NiFBrS_4$: C, 38.67; H, 1.78; N, 13.53. Found: C, 38.62; H, 1.85; N, 13.37%. Infrared spectrum (cm^{-1}): ν(N–H), 3378.8 s, 1652.0 s, ν(CN) 2205.8 s, ν(C=C) of mnt^{2-}, 1452.6 s. The black single crystals suitable for the X-ray structure analysis were obtained by evaporating the MeCN and *i*-PrOH (v/v = 1:1) mixed solution of **1** about two weeks at room temperature. Elemental analyses were run on a Model 240 Perkin–Elmer CHN instrument. IR spectra were recorded on an IF66V FT-IR (400–4000 cm^{-1} region) spectrophotometer in KBr pellets. Magnetic susceptibility data on crushed polycrystalline sample of **1** were collected over the temperature range of 2–300 K using a Quantum Design MPMS-5S super-conducting quantum interference device (SQUID) magnetometer, and diamagnetic corrections were made using Pascal's constants. Crystallographic details of **1** are listed in Table 1.

Table 1
Crystal data and structure refinement for **1**

Temperature (K)	293(2)
Empirical formula	$C_{20}H_{11}N_6NiBrFS_4$
Formula weight	621.22
Wavelength	0.71073 Å
Crystal system	Monoclinic
Space group	$P2_1/c$
Unit cell dimensions	
a (Å)	11.848(4)
b (Å)	26.611(8)
c (Å)	7.744(10)
β (°)	100.64(1)
Volume (Å^3), Z	2400(3), 4
Density (calculated) (mg/m^3)	1.720
Absorption coefficient (mm^{-1})	2.851
F(000)	1236
Crystal size (mm^{-1})	0.4 × 0.2 × 0.2
θ range for data collection	1.91–26.00
Limiting indices	$-14 \leqslant h \leqslant 12$, $-32 \leqslant k \leqslant 29$, $-9 \leqslant l \leqslant 9$
Reflections collected	12619
Independent reflections	4683 (R_{int} = 0.085)
Refinement method	Full-matrix least-squares on F^2
Data/restraints/parameters	4683/0/299
Goodness of fit on F^2	0.99
Final R indices ($I > 2\sigma(I)$)	R_1 = 0.0421, wR_2 = 0.0838
R indices (all data)	R_1 = 0.0613, wR_2 = 0.0855
Largest diff. peak and hole e Å^{-3}	0.48 and −0.86

3. Results and discussion

3.1. Description of structure of *1*

Complex **1** crystallizes in the monoclinic space group $P2_1/c$. The structure and an ORTEP drawing with non-hydrogen atomic labeling of the asymmetric are shown in Fig. 1. Selected bond lengths and bond angles are listed in Table 2. The molecular structure of the $Ni(mnt)_2^-$ anion consists of two mnt^{2-} ligands symmetrically chelated to the nickel cation which adopts the expected square–planar coordination geometry. The Ni–S bond distances and the S–Ni–S bond angles within the five-membered rings compare well with those found in $Ni(mnt)_2^-$ complexes [13]. The CN groups of $Ni(mnt)_2^-$ anion are slightly tipped out of the plane; the deviations from the plane are −0.4606 Å for N(1), −0.5102 Å for N(2), −0.1654 Å for N(3) and 0.2850 Å for N(4). The $[BrFBzNH_2Py]^+$ cation adopts a conformation, where

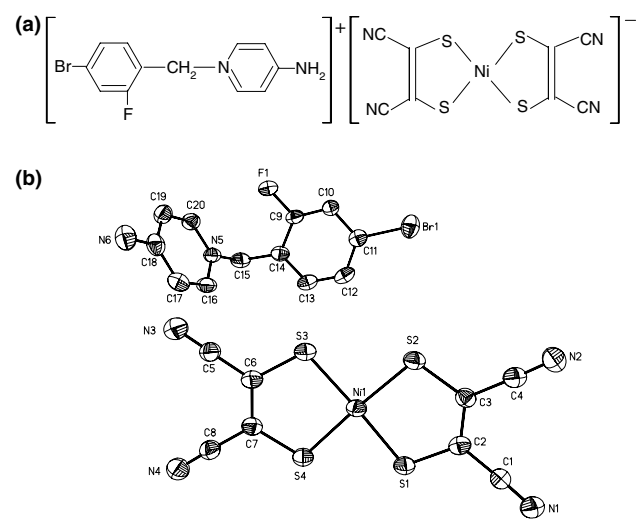

Fig. 1. (a) The structure of **1**. (b) ORTEP plot (30% probability ellipsoids) showing the molecule structure of **1**.

Table 2
Selected bond lengths, bond angles and intermolecular contacts for **1**

Bond lengths (Å)			
Ni(1)–S(1)	2.142(3)	Ni(1)–S(2)	2.153(3)
Ni(1)–S(3)	2.149(3)	Ni(1)–S(4)	2.133(3)
Bond angles (°)			
S(1)–Ni(1)–S(2)	92.47(4)	S(3)–Ni(1)–S(4)	92.38(4)
S(1)–Ni(1)–S(4)	85.23(4)	S(2)–Ni(1)–S(3)	89.89(4)
Intermolecular contacts (Å)			
Ni(1)···Ni(1)^a	4.045	S(1)···S(4)^a	3.791
Ni(1)···Ni(1)^b	4.045	Br(1)···C(9)^a	3.746
Ni(1)···S(4)^a	3.753	Br(1)···C(13)^b	3.853
Ni(1)···S(4)^b	3.753	Br(1)···C(14)^b	3.766

Symmetry codes: $a = x, 0.5 - y, 0.5 + z$; $b = -1 + x, y, z$.

both the phenyl ring and pyridine ring are twisted to the C(14)–C(15)–N(5) reference plane. The dihedral angles that pyridine ring and phenyl ring make with the reference plane are 80.6° and 106.8°, respectively. An interesting structural features of **1** is the presence of the completely segregated uniform stack columns of $Ni(mnt)_2^-$ anions and $[BrFBzNH_2Py]^+$ cations, each flanked by two columns of cations, as revealed by the projection along the crystallographic *c*-axis in Fig. 2a. The Ni···Ni distance is 4.045 Å in the $Ni(mnt)_2^-$ anions stacking column; the nearest Ni···S and S···S distances are 3.679 and 3.791 Å. While the closest Ni···Ni separation between anion columns is 13.459 Å, which is significantly longer than the distance of Ni···Ni separation within a column. Obviously, there exist intermolecular interactions between neighboring $Ni(mnt)_2^-$ anions within an anion column. Therefore, each $Ni(mnt)_2^-$ anion can be considered as a quasi-one-dimensional uniform magnetic chains through the shorter intermolecular interactions from the viewpoint of the crystal structure.

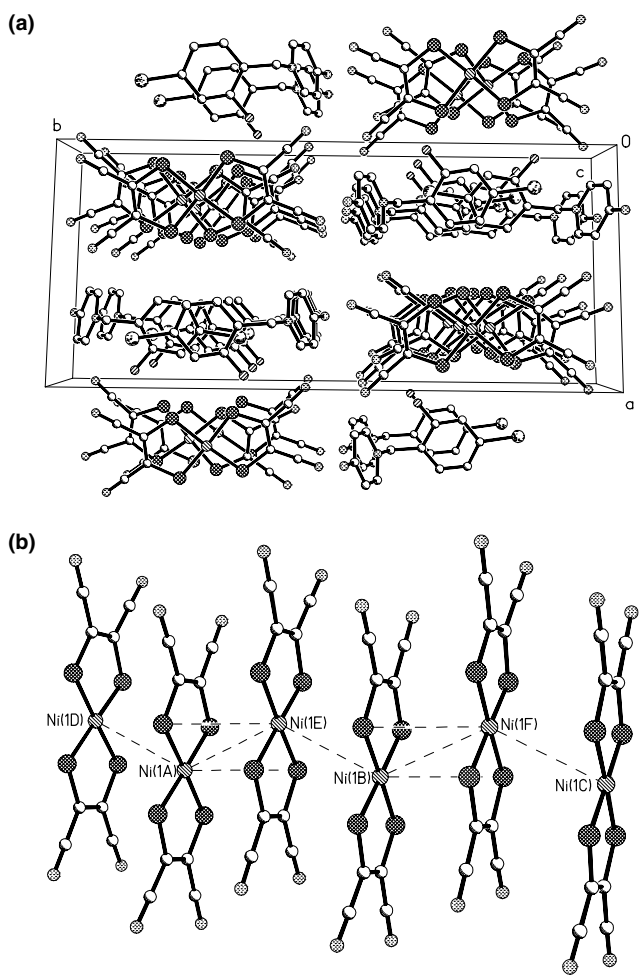

Fig. 2. (a) The packing diagram of a unit cell for **1** as viewed along *c*-axis. (b) Side view of the anions stack of **1** showing the uniform space linear-chain of $[Ni(mnt)_2]^-$.

The slipped zig–zag configuration of $Ni(mnt)_2^-$ anions are displayed in Fig. 2b. The $[BrFBzNH_2Pyl]^+$ cations orient themselves in the solid state and also form a 1D chain through p–π interactions between Br atom and the neighboring phenyl rings duo to the shorter intermolecular separations occurring between Br(1) and C(9)[a], Br(1) and C(13)[b], Br(10) and C(14)[b] of adjacent benzene rings. This p–π interaction between the halogen atoms and the benzene rings has also been found in some halogeno-benzene derivatives in the solid state [10,14–16]. It is worth noting that the intermolecular hydrogen bonds between anions and cations were observed in crystal structure and molecular structure. The intermolecular contact is N(6) atom with the N(2)($1 - x$, $1/2 + y$, $-1/2 - z$) and N(4)($1 - x$, $1 - y$, $-z$) atom being 3.028(7) and 3.151(6) Å, respectively. The hydrogen atom associated with these atoms has the following contacts with N(6)···H(6) 2.590 and 2.490 Å. These contacts play important roles in crystal packing and stability of **1**.

3.2. Magnetic properties

Variable-temperature (2–300 K) magnetic susceptibility data is collected on crushed polycrystals of **1**. The temperature dependent of the χ_m, measured under a field of 1000 Oe, are shown in Fig. 3a. As the temperature is lowered, the χ_m varies in a complex way: it first increases smoothly a maximum at 20 K, then decreases abruptly to a rounded minimum at 10 K, and finally increases again upon further cooling to 2 K. It is worthy to note that the χ_m vs. T curve undergoes an inflection around 10 K. The room temperature $\chi_m T$, value of 0.372 emu K mol^{-1} is in good agreement with the expected value for Ni^{III} ($S = 1/2$) that are magnetically isolated (expected value is 0.375 emu K mol^{-1}). On cooling down, the $\chi_m T$ increases gradually and reaches a maximum of 0.742 emu K mol^{-1} at 20 K. This behavior indicates the ferromagnetic interactions between the metal spin centers in this temperature range. This origin of the ferromagnetic interaction can be illustrated by means of McConnell's theory because the structure of **1** meets two conditions of magnetic coupling [8,17]. The magnetic susceptibility data at 20–300 K for **1** are best fit by the Baker equation for a 1D magnetic chain with $S = 1/2$ spin [18,19]. Eq. (1) for $H = -2\sum S_i S_j$, with $y = J/2kT$

$$\chi_m = \frac{Ng^2\beta^2}{4kT}\left[\frac{C}{D}\right]^{2/3}, \tag{1}$$

where $C = 1.0 + 5.79799y + 16.902653y^2 + 29.376885y^3 + 29.832959y^4 + 14.036918y^5$ and $D = 1.0 + 2.797991y + 7.0086780y^2 + 8.653844y^3 + 4.5743114y^4$.

A fit of the data to Eq. (1) gives $J = 0.42$ cm^{-1} and $g = 2.26$, TIP $= 1.4 \times 10^{-4}$ emu mol^{-1} with a final

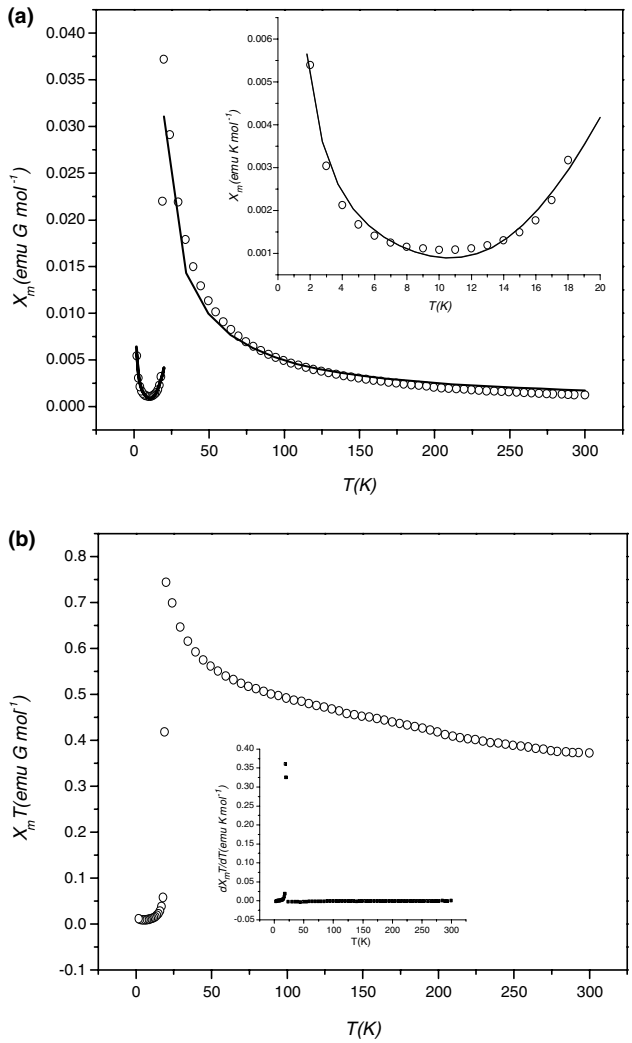

Fig. 3. (a) Plot of χ_m vs. T for **1**. The solid line are reproduced from the theoretic calculations and detailed fitting procedure described in the text. (b) The plot of $\chi_m T$ vs. T for **1** (inset: $d(\chi_m T)/dT$ vs. T).

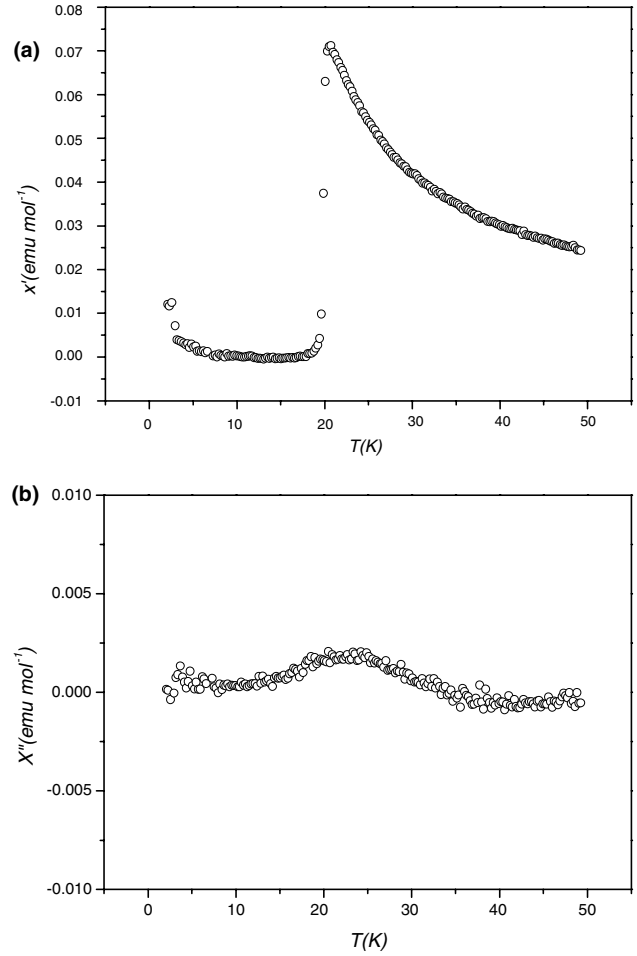

Fig. 4. In-phase (a) and out-phase (b) components of the a.c. susceptibilities for **1** at 1633 Hz.

agreement factor $R = 2.1 \times 10^{-4}$ (R is defined as $\sum(\chi_m^{calc} - \chi_m^{obsd})^2/(\chi_m^{obsd})^2)$, which is in agreement with the ferromagnetic coupling between adjacent $S = 1/2$ Ni spin carriers within the anion chain of **1** mentioned above.

In the low-temperature phase (2–20 K), the $\chi_m T$ decreases exponentially and drops from 0.742 emu K mol^{-1} at 20 K to a minimum of 0.00837 emu K mol^{-1} at about 5 K as the sample temperature decreases, and exhibits the characteristics of a spin gap system. The transition temperature, 20 K, may be estimated from the $d(\chi_m T)/dT$ vs. T plot (the inset of Fig. 3b). The magnetic susceptibility may be estimated by the formula $\chi_m = [\alpha \exp(-\Delta/k_B T)]/T + C/T + \chi_0$, where α is a constant value corresponding to the dispersion of excitation energy, Δ is the magnitude of the spin gap, χ_0 contributes from the core diamagnetism and the possible Van Vleck paramagnetism, and the other symbols have their usual meaning. The best fit curve for **1** is shown in Fig. 3a, and the corresponding parameters are given as follows: $\alpha = 7.71$, $\Delta/k_b = 92.0$ K, $\chi_0 = 2.3 \times 10^{-4}$ emu mol^{-1}, $C = 1.06 \times 10^{-2}$ emu K mol^{-1}, and $R = 4.5 \times 10^{-8}$ (R is defined as $\sum(\chi_m^{calcd} - \chi_m^{obsd})^2/(\chi_m^{obsd})^2)$. According to the results, the values of the parameter $2\Delta/k_b T_c$ (T_c is the transition temperature) are estimated to be 9.20 for **1**, which is higher than the ideal value of 3.53 derived from the BCS formula in a weak coupling regime. This result thus means that the short-range magnetic correlations within a chain are not fully developed and intrinsic magneto elastic instability of a 1D system cannot be considered as a driving force for this transition; namely, the transition is not a pure Spin-Peierls transition [10]. The origins of the phase transition for **1** are attributed to cooperative interactions of Ni···S bonding, inter-plane repulsion of the $[Ni(mnt)_2]^-$ anions [20], π···π stacking interactions between of adjacent cations, spin-lattice interaction [21] and spin–spin coupled interaction between nearest-neighbor anions [22].

To further determine the precise temperature of magnetic transition, ac magnetic susceptibility measure-

ments are performed. In **1**, χ' shows a maximum and the peak (Fig. 4a) is very sharp at 20.75 K (1633 Hz), indicating there exists effective magnetic transition but not be suggests as the ferromagnetic ordering temperature. It can be confirmed by the linear relationship of M vs. H (Fig. 5a). Usually, in a magnet containing net magnetic moments in ordered state, there is a maximum in the in-phase signal (χ') near T_c, and the out-of-phase signal (χ'') appears at the temperature just below T_c. But in **1**, a rounded maximum of nonzero χ'' was found at around 21.6 K (Fig. 4b). The increases of χ' and χ'' values below around 5 K as the temperature is lowered, confirming the occurrence of another magnetic phase transition suggested by dc magnetic measurements. The field-dependent magnetization of **1** was measured at 19.7 K (Fig. 5a); the magnetization at the highest measured field (70 kG) is 2123 emu mol^{-1}, which is below the theoretical saturation value 5585 emu mol^{-1}. The linearity of the curve is consistent with the presence of short-range magnetic ordering.

The final increase of the magnetic susceptibility at very low temperature (5 K) may due to the presence of weak ferromagnetic interaction of **1**. To get a closer characterization in the low-temperature region, the field-dependent magnetization of **1** at 2 K measured under different fields (Fig. 5b). The magnetization increases very rapidly before the field reaches 10 kG, above which the magnetization saturates rapidly upon increasing the field. The saturation magnetization is 16.34 emu G mol^{-1}, far below the saturation value (5585 emu mol^{-1}) expected for an $S = 1/2$ system, consistent with weak ferromagnetism duo to spin canting (the small canting angle α is about 0.17° deduced from $\sin\alpha = M_w/M_s$). Spin canting arises through a Dzyaloshinsky–Moriya interaction [23–26], which minimizes the coupling energy when two spins are perpendicular to one another, and this magnitude is proportional to $\Delta g/g$. The results of the structural analysis in the room temperature of **1** indicate that a symmetric element is present in a $P2_1/c$ space group; the antisymmetric exchange is excluded as a factor accounting for the spin canting. So only the local anisotropy would account for the magnetic behavior observed. No hysterisis hoop was observed at 2 K.

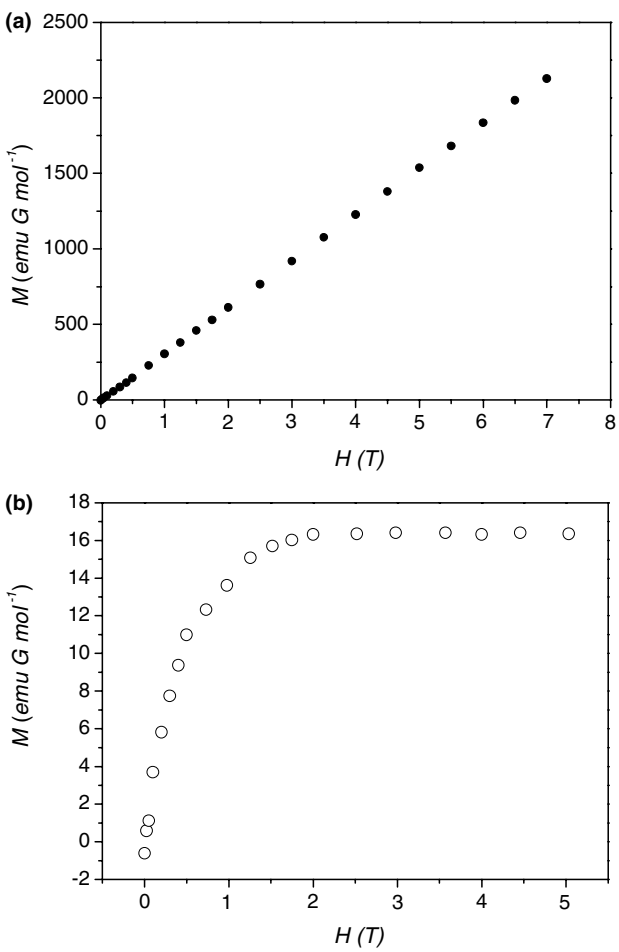

Fig. 5. Magnetization vs. H for **1** at the temperature of 19.7 K (a) and 2 K (b).

4. Conclusion

The crystal structure of **1** at room temperature illustrate that the $Ni(mnt)_2^-$ anions and $[BrFBzNH_2Py]^+$ cations of **1** posses well-separated stacking column. The $Ni(mnt)_2^-$ anions form a 1D completely segregated uniform magnetic chains through intermolecular S···S, Ni···Ni, S···Ni, or π···π interactions. The measurements of the temperature dependence of magnetic susceptibility for **1** in the temperature range 2–300 K reveal the occurrence of significant ferromagnetic interaction in the high-temperature phase (HT), spin-gapped system in the low-temperature phase (LT), and weak ferromagnetism due to spin canting below 5 K.

5. Supplementary material

Supplementary crystallographic data are available from the Cambridge Crystallographic Data Center, CCDC No. 242815. Copies of this information may be obtained free of charge from The Director, CCDC, 12 Union Road, Cambridge, CB2 1EZ, UK (fax: +44 1223 336033; deposit@ccdc.cam.ac.uk or www: http://www.ccdc.cam.ac.uk).

Acknowledgements

The authors are grateful for financial support from the National Natural Science Foundation of China (Project No. 20171022). The Center of Analysis and Determination of Nanjing University are acknowledged.

References

[1] E. Coronado, J.R. Galan-mascaros, C.J. Gomez-Garcia, V. Laukhin, Nature 408 (2000) 447.
[2] E. Coronado, F. Palacio, J. Veciana, Angew. Chem. Int. Ed. 42 (2003) 2570.
[3] E. Canadell, Coord. Chem. Rev. 185–186 (1999) 629.
[4] N. Robertson, L. Cronin, Coord. Chem. Rev. 227 (2002) 93.
[5] M. Urichi, K. Yakushi, Y. Yamashita, J. Qin, J. Mater. Chem. 8 (1998) 141.
[6] P.I. Clemenson, A.E. Underhill, M.B. Hursthouse, R.L. Short, J. Chem. Soc., Dalton Trans. (1988) 1689.
[7] J.F. Weiher, L.R. Melby, R.E. Benson, J. Am. Chem. Soc. 86 (1964) 4329.
[8] A.T. Coomber, D. Beljonne, R.H. Friend, J.L. Brédas, A. Charlton, N. Robertson, A.E. Underhill, M. Kurmoo, P. Day, Nature 380 (1996) 144.
[9] J.L. Xie, X.M. Ren, Y. Song, W.W. Zhang, W.L. Liu, C. He, Q.J. Meng, Chem. Commun. (2002) 2346.
[10] X.M. Ren, Q.J. Meng, Y. Song, C.S. Lu, C.J. Hu, Inorg. Chem. 41 (2002) 5686.
[11] S.B. Bulgarevich, D.V. Bren, D.Y. Movshovic, P. Finocchiaro, S. Failla, J. Mol. Struct. 317 (1994) 147.
[12] A. Davison, R.H. Holm, Inorg. Synth. 10 (1967) 8.
[13] K. Brunn, H. Endres, J. Weiss, Z. Naturforsch. 42B (1987) 1222.
[14] M.R. Sundberg, R. Sillanpää, Acta Chem. Scand. 46 (1992) 34.
[15] R. Sillanpää, J. Jokela, M.R. Sundberg, Inorg. Chem. 36 (1997) 3301.
[16] M.R. Sundberg, Inorg. Chim. Acta 267 (1998) 249.
[17] H.M McConnell, J. Chem. Phys. 39 (1963) 1910.
[18] G.A. Baker, G.S. Rushbrooke, H.E. Gilbert, Phys. Rev. 135 (1964) A1272.
[19] L. Deakin, A.M. Arif, J.S. Miller, Inorg. Chem. 38 (1999) 5072.
[20] S. Alvarez, R. Vicente, R. Hoffmann, J. Am. Chem. Soc. 107 (1985) 6253.
[21] E. Pytte, Phys. Rev. B 10 (1974) 4637.
[22] M.E. Itkis, X. Chi, A.W. Cordes, R.C. Haddon, Science 296 (2002) 1443.
[23] S.R. Batten, P. Jensen, C.J. Kepert, M. Kurmoo, B. Moubaraki, K.S. Murray, D.J. Price, J. Chem. Soc., Dalton Trans. (1999) 2987.
[24] S.J. Rettig, R.C. Thompson, J. Trotter, S. Xia, Inorg. Chem. 38 (1999) 1360.
[25] X.M. Ren, Y.C. Chen, C. He, S. Gao, J. Chem. Soc., Dalton Trans. (2002) 3915.
[26] E.Q. Gao, Y.F. Yue, S.Q. Bai, Z. He, C.H. Yao, J. Am. Chem. Soc. 126 (2004) 1419.